Investigating the Impact of Higher-Order Phase Transitions in Binary Neutron-Star Mergers

Peter Hammond

Albert Einstein Institute, Potsdam

Collaborators: Alex Clevinger, Milena Albino, Veronica Dexheimer, David Radice, et al.

arXiv:2508.10698, see also arxiv:2506.24069

peter.hammond@aei.mpg.de

6th February, 2026

Quarks in BNS mergers

- Simulations have suggested that the QCD phase transition may leave a measurable imprint on GWs from BNS mergers.
- See e.g. Most et al. 2019; Bauswein et al. 2019; Prakash et al. 2024; Espino et al. 2024 etc..
- These works focus on first-order phase transitions, but higher orders are possible.

Higher order PTs

- We start with three (barotropic) EoSs that feature a first order phase transition from hadrons to quarks:
  - CMF-2 *
  - CMF-7 *
  - RDF 1.7 *
- We use *percolation* to replace the phase transition.
- Any order is possible, however here we focus mostly on second ($p(\mu_{\mathrm{B}})$ is $\mathcal{C}^1$) and third ($p(\mu_{\mathrm{B}})$ is $\mathcal{C}^2$) order transitions.
- ($\mathcal{C}^1 \Rightarrow$ pressure is continuous and smooth but c_s^2 is discontinuous, $\mathcal{C}^2 \Rightarrow c_s^2$ also continuous)

* CompOSE link

Percolation

- The percolation of the EoSs is performed by replacing $p(\mu_{\mathrm{B}})$ over some chosen interval with a polynomial $\mathcal{P}$ of the form

$$\mathcal{P}(\mu_{\mathrm{B}}) = \sum_{m=0}^{M} b_m \mu_{\mathrm{B}}^m = b_0 + b_1 \mu_{\mathrm{B}} + b_2 \mu_{\mathrm{B}}^2 + b_3 \mu_{\mathrm{B}}^3 + ...$$

- The coefficients b_m are fixed by matching the value and derivatives of $\mathcal{P}$ to $p(\mu_{\mathrm{B}})$ (or imposing chosen values) at the interval boundaries.
- Here we focus on 5^{th} degree polynomials, and parameter choices that increase the maximum TOV mass of the EoS.

Percolation

- The resulting EoSs have 3 phases—a hadronic phase, a percolated phase, and a pure quark phase.
- The low and high density parts of each EoS are unchanged.
- The percolated phase does not represent a mix of the two other phases.
- This model gives us a lot of freedom w.r.t. the phase transitions and the resulting EoSs.

Modified Equations of State

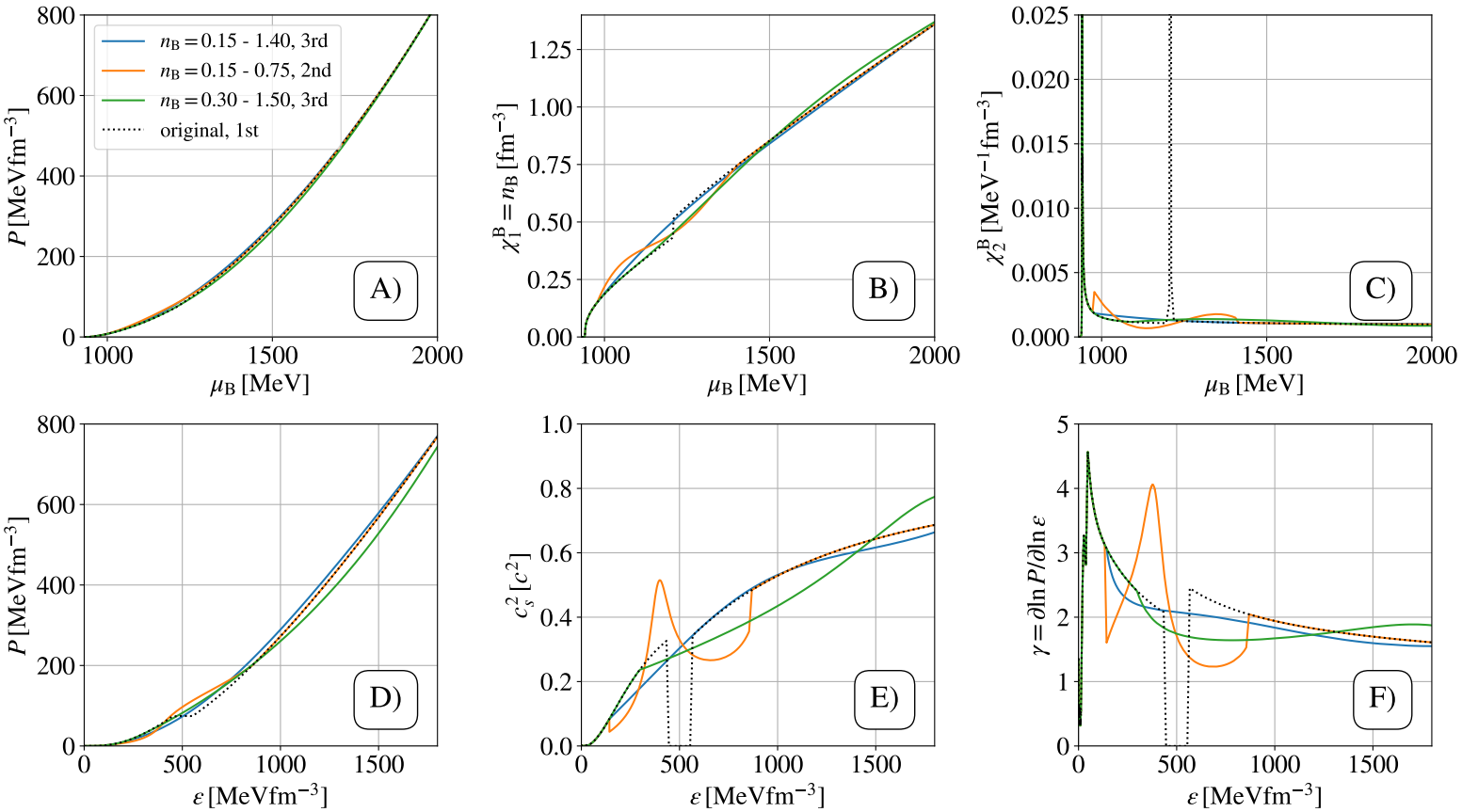

Figure 1: Base CMF-2 equation of state, and several percolated versions.

Modified Equations of State

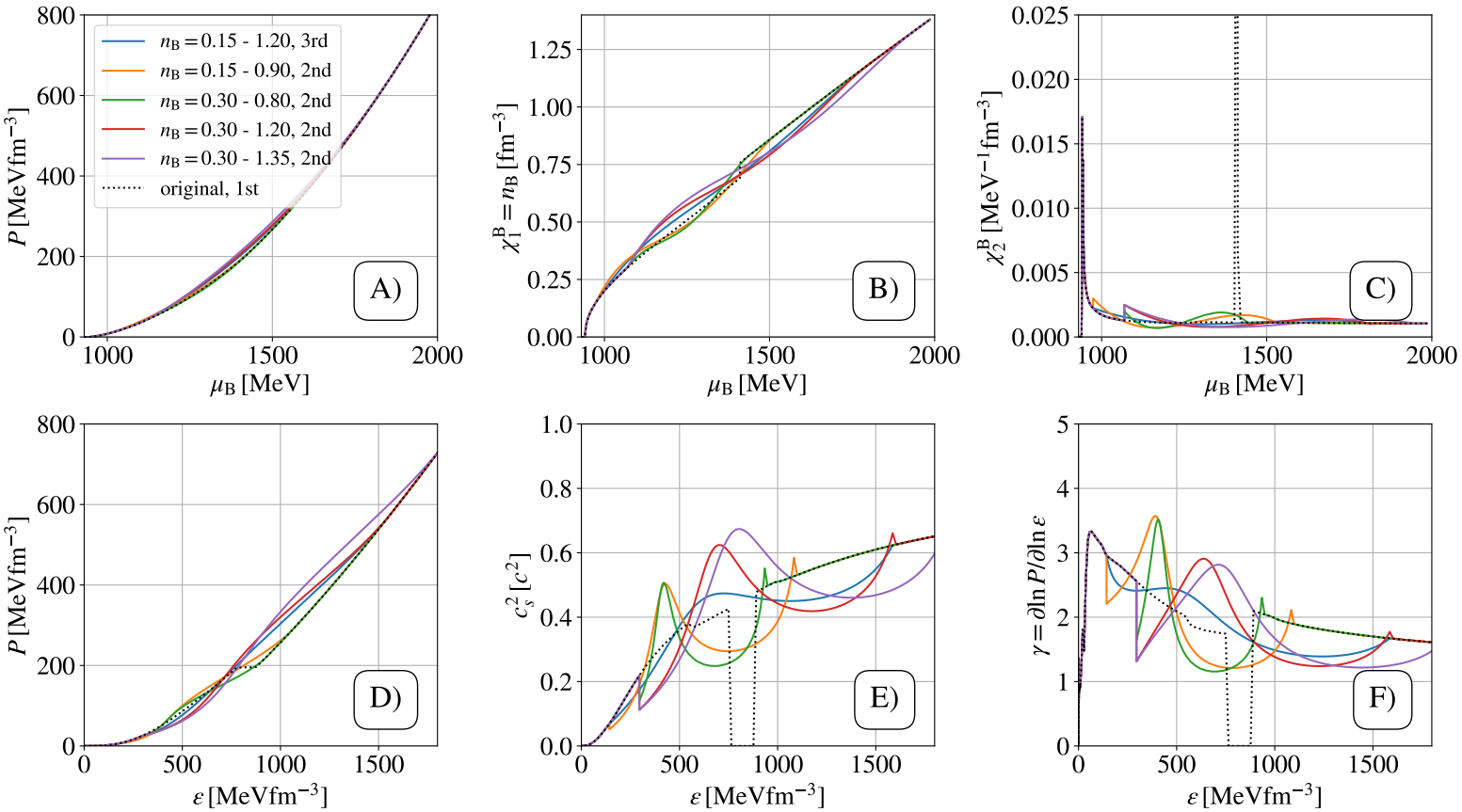

Figure 2: Base CMF-7 equation of state, and several percolated versions.

Modified Equations of State

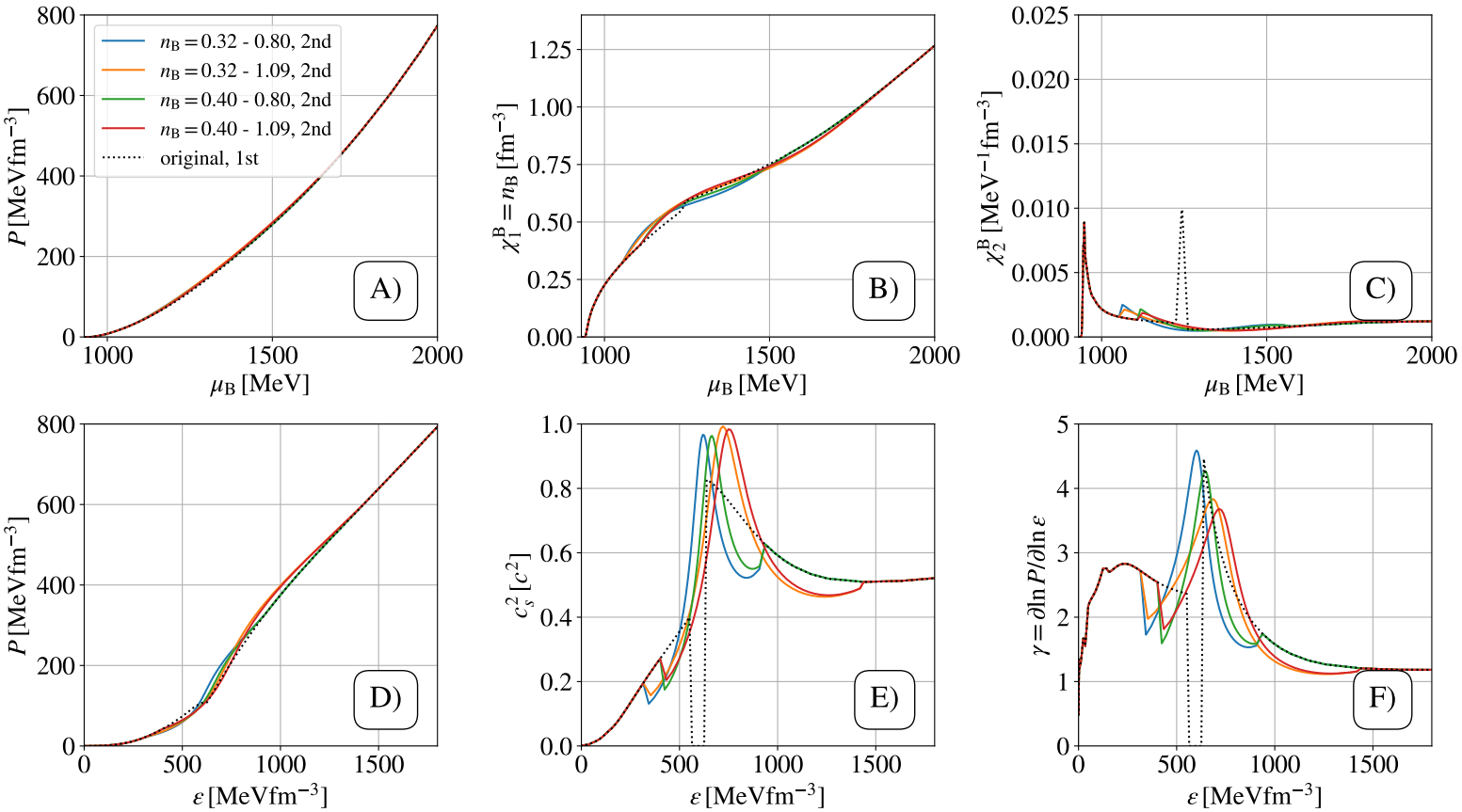

Figure 3: Base RDF 1.7 equation of state, and several percolated versions.

Speed of sound bump

- The existence of $\geq 2\,M_\odot$ neutron stars (e.g. Antoniadis et al. 2013) implies a stiff dense matter EoS.
- Radius (e.g. Miller et al. 2019) and tidal deformability (e.g. Abbott et al. 2018) measurements imply a softer EoS at lower densities.
- pQCD predicts a small c_s^2 at asymptotically high densities (e.g. Fraga et al. 2014).
- Together, these constraints imply a bump in c_s^2 (e.g. Tews et al. 2018), which these percolated EoSs qualitatively reproduce.

Mass - Radius

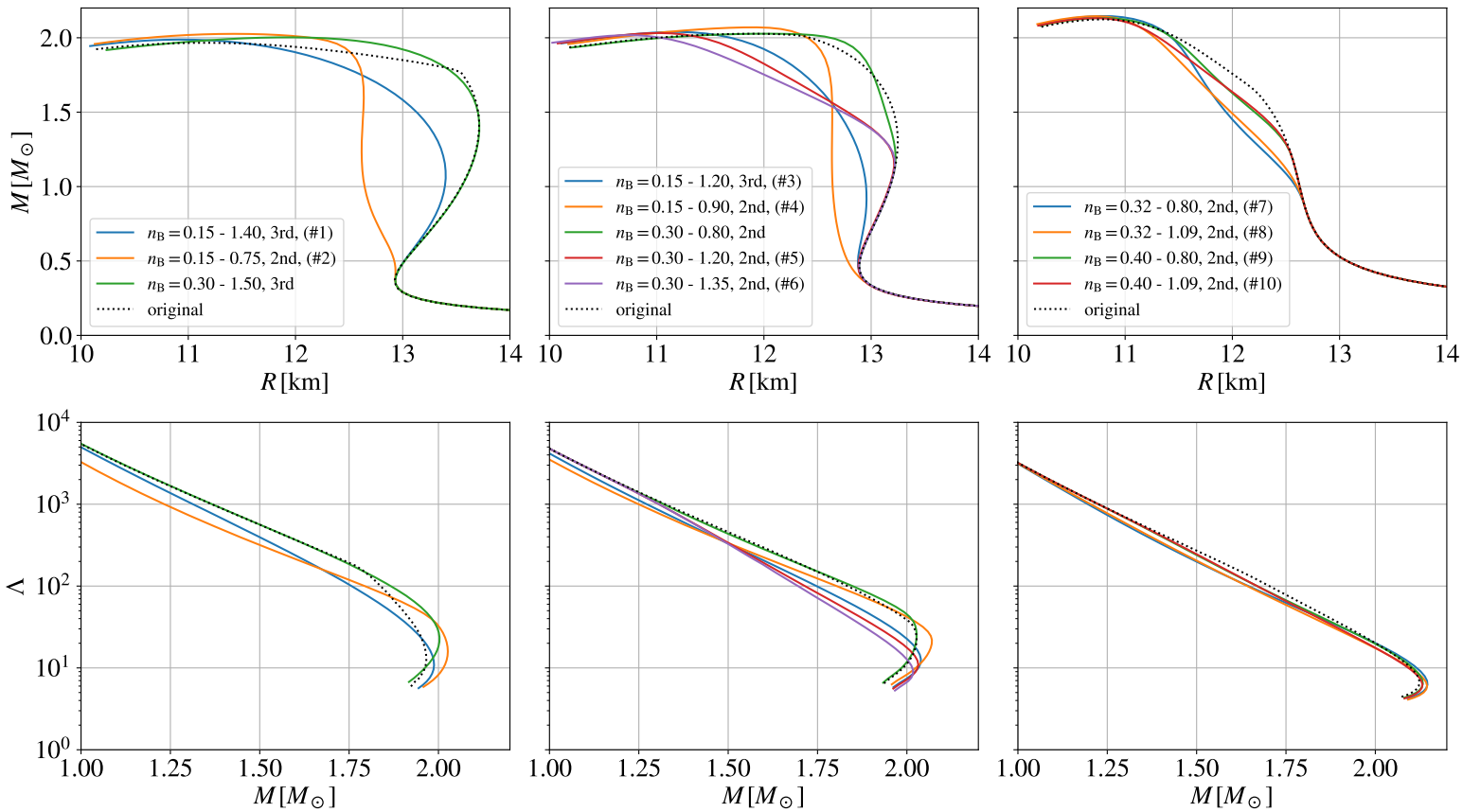

Figure 4: Mass-radius curves and mass-tidal deformability (Λ) curves for considered EoSs.

Simulations

- We use the GR-Athena++ code (Cook et al. 2023; Daszuta and Cook 2024 etc.).
- This code features octree based AMR, Z4c spacetime evolution, and Valencia-based GRMHD.
- The percolation prescription is barotropic, so we are limited to 1D tables.
- The 1D tabulated EoSs are supplemented with a gamma-law thermal component.
- We use a fiducial resolution of $\sim$185 m ($0.125\,M_\odot$).

Pressure - Density

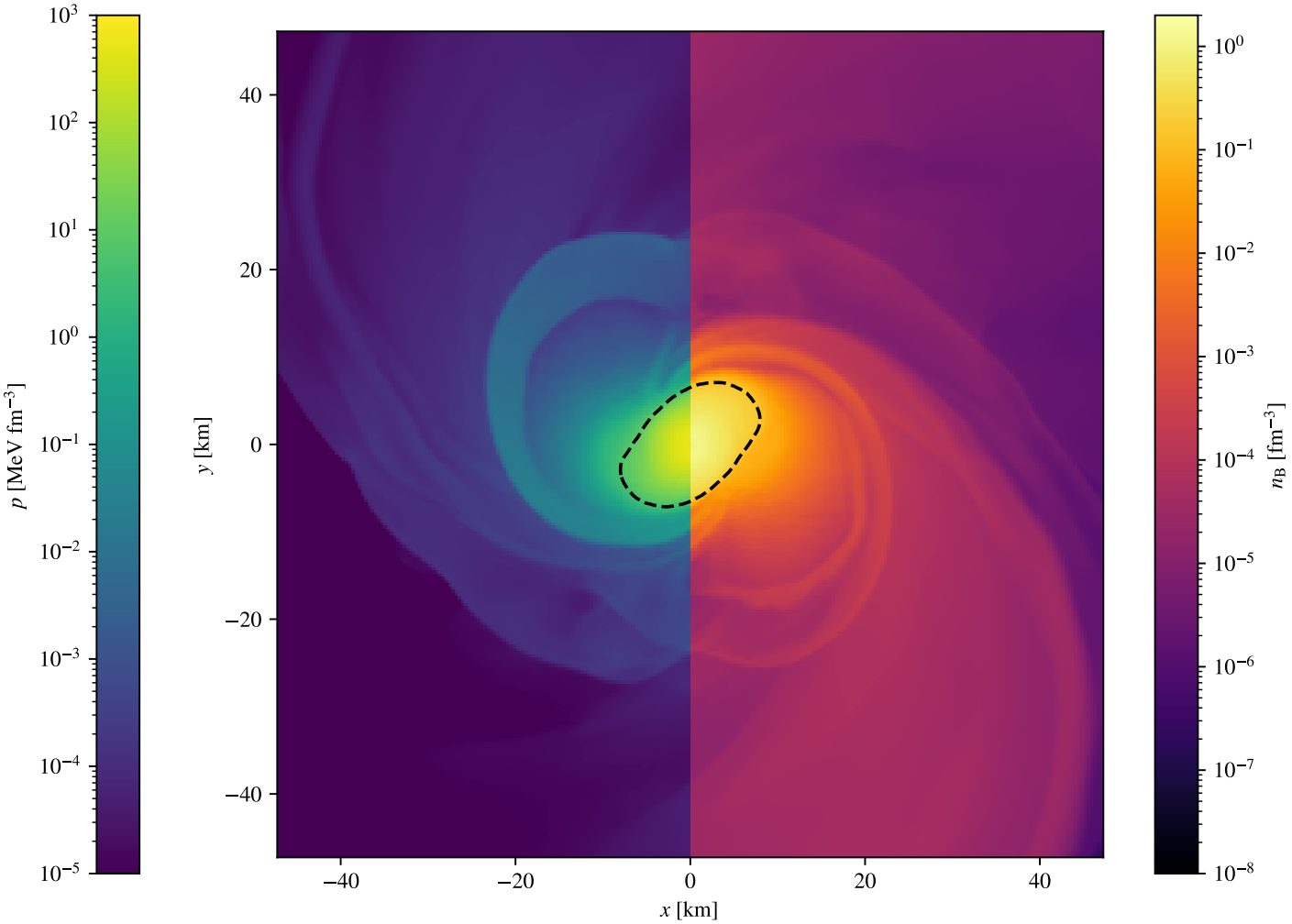

Figure 5: Pressure and density shortly before collapse for CMF-7 model 1 (Sim 3). Dashed density contour shows beginning of percolated region.

Pressure - Density

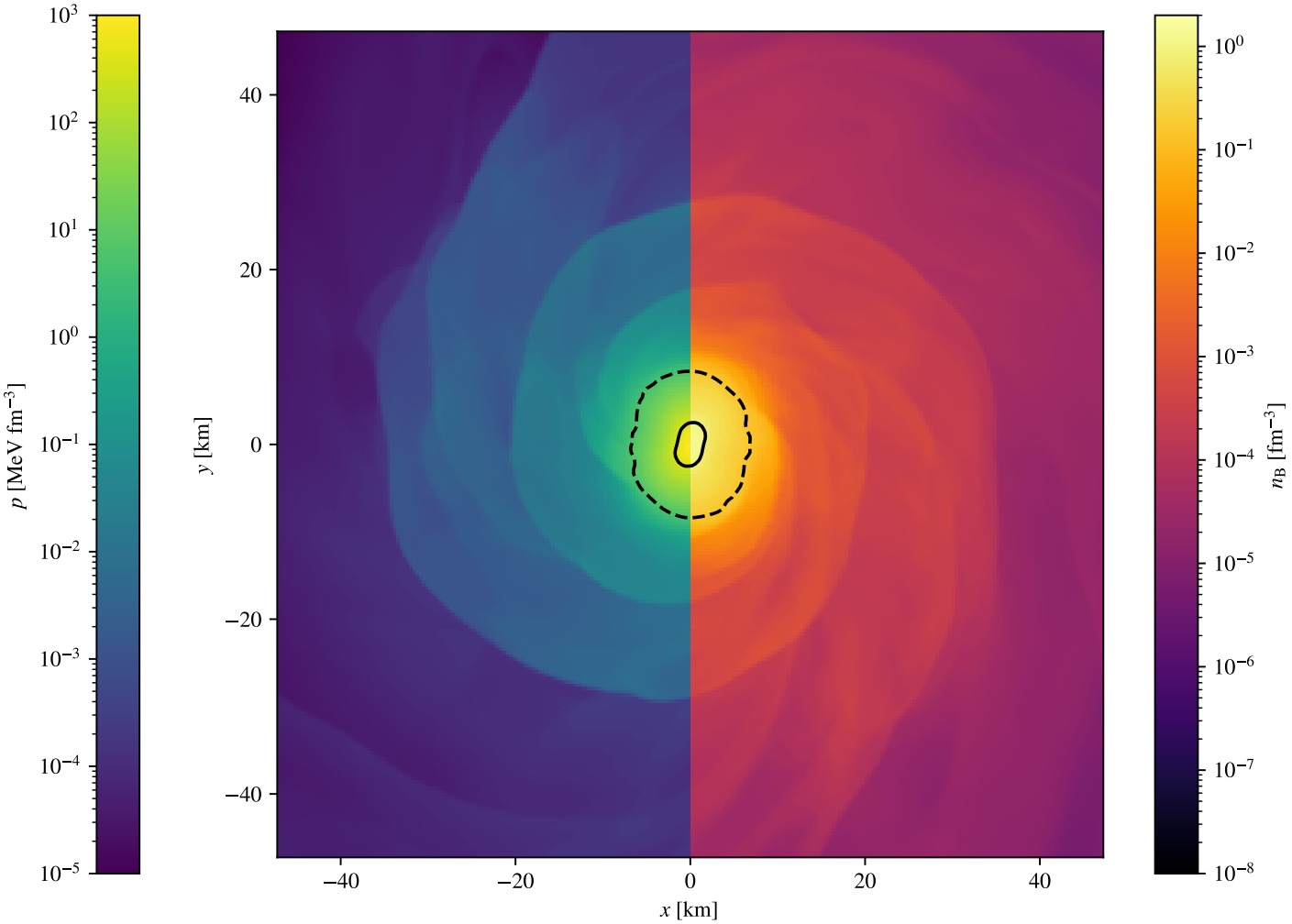

Figure 6: Pressure and density shortly before collapse for CMF-7 model 2 (Sim 4). Dashed density contour shows beginning of percolated region, solid contour shows beginning of pure quark region.

GW Strain

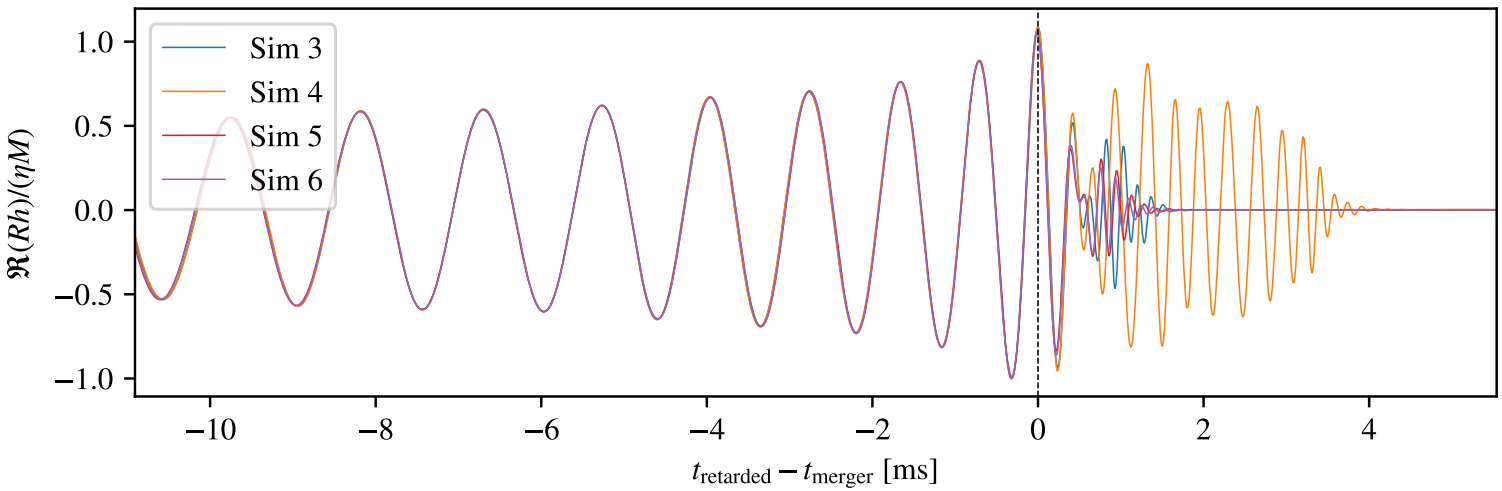

Figure 7: Real part of GW strain for selected CMF-7 models.

GW Strain

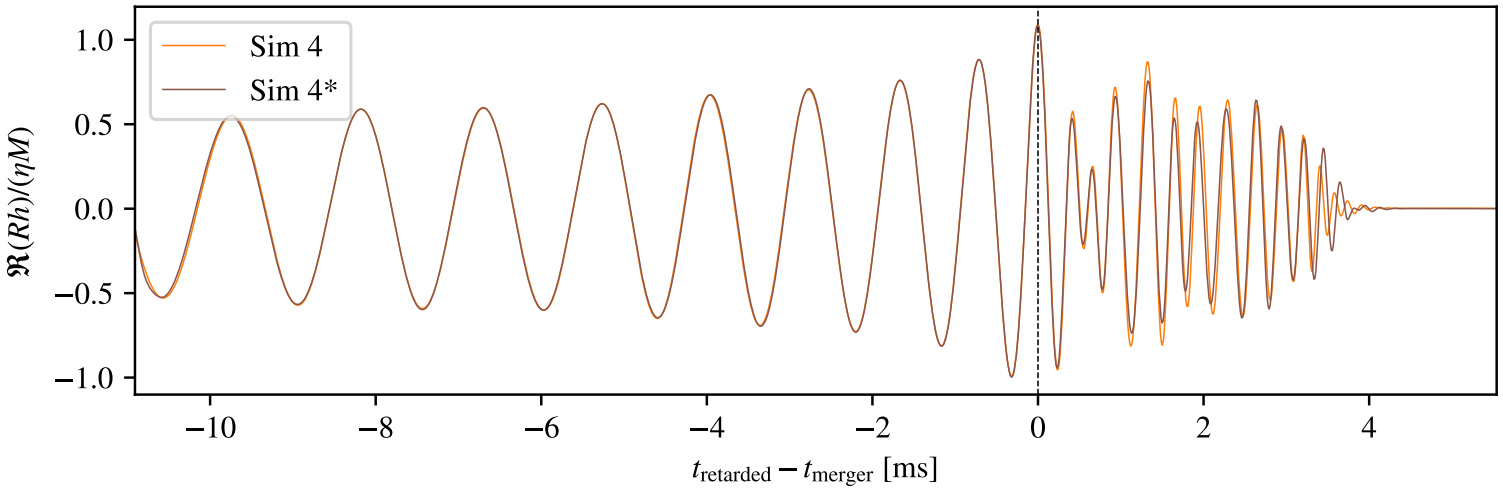

Figure 8: Real part of GW strain for CMF-7 model 2 (Sim 4) at fiducial resolution (∼185 m) and 25% reduced resolution (∼230 m, Sim 4*).

GW Spectra

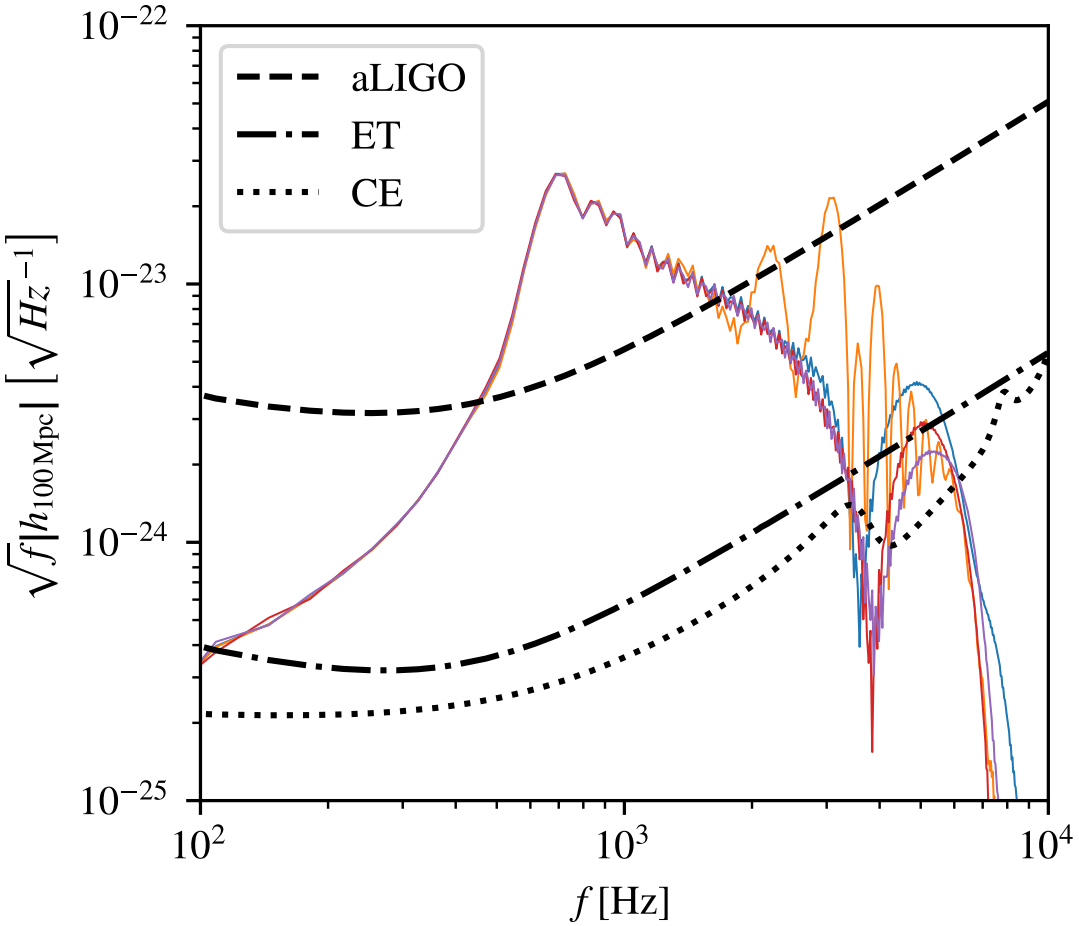

Figure 9: GW amplitude spectral density at a distance of 100 Mpc for selected CMF-7 models. Detector sensitivity curves for ALIGO (dashed), ET (dash-dotted), and CE40km (dotted) are shown for comparison.

GW Spectra

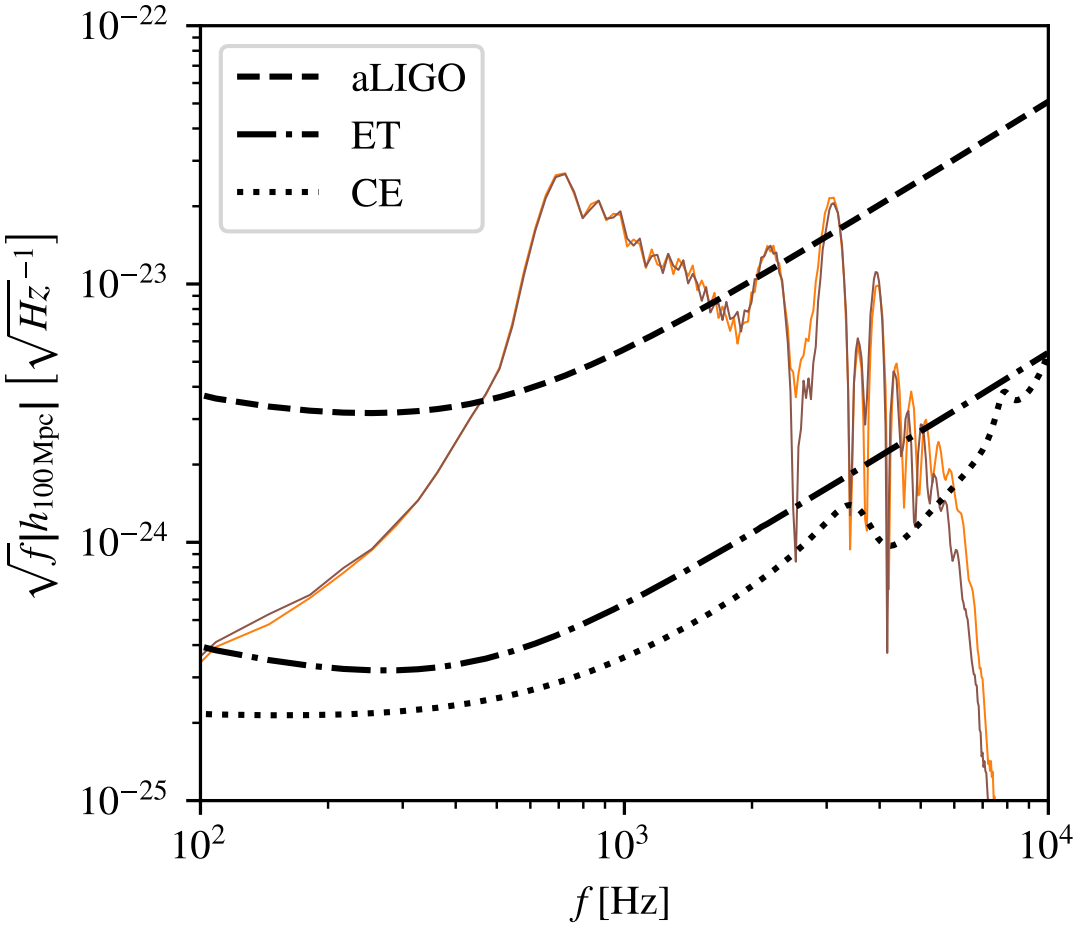

Figure 10: GW amplitude spectral density at a distance of 100 Mpc for CMF-7 model 2 (Sim 4) and low resolution simulation of same EoS model (Sim 4*).

Mismatch

- We can compute the mismatch, $\mathcal{M}$, between two wavefoms as

$$\mathcal{M} = 1 - \max_{\phi_c, t_c} \frac{\left\langle \tilde{h}_1(f) | \tilde{h}_2(f) e^{i(\phi_c - 2\pi f t_c)} \right\rangle}{\sqrt{\left\langle \tilde{h}_1(f) | \tilde{h}_1(f) \right\rangle \left\langle \tilde{h}_2(f) | \tilde{h}_2(f) \right\rangle}},$$

  where

$$\left\langle \tilde{h}_1(f) | \tilde{h}_2(f) \right\rangle = 4 \int_0^\infty \frac{\tilde{h}_1^*(f) \tilde{h}_2(f)}{S_n(f)} \mathrm{d}f,$$

  ϕ_c and t_c are, respectively, the phase and time shifts, and S_n is the detector sensitivity.
- In our calculations we use the ET-D noise curve.
- Additionally, we can restrict the integral above to only consider frequencies $f \geq f_{\text{merger}}$.

Merger frequency

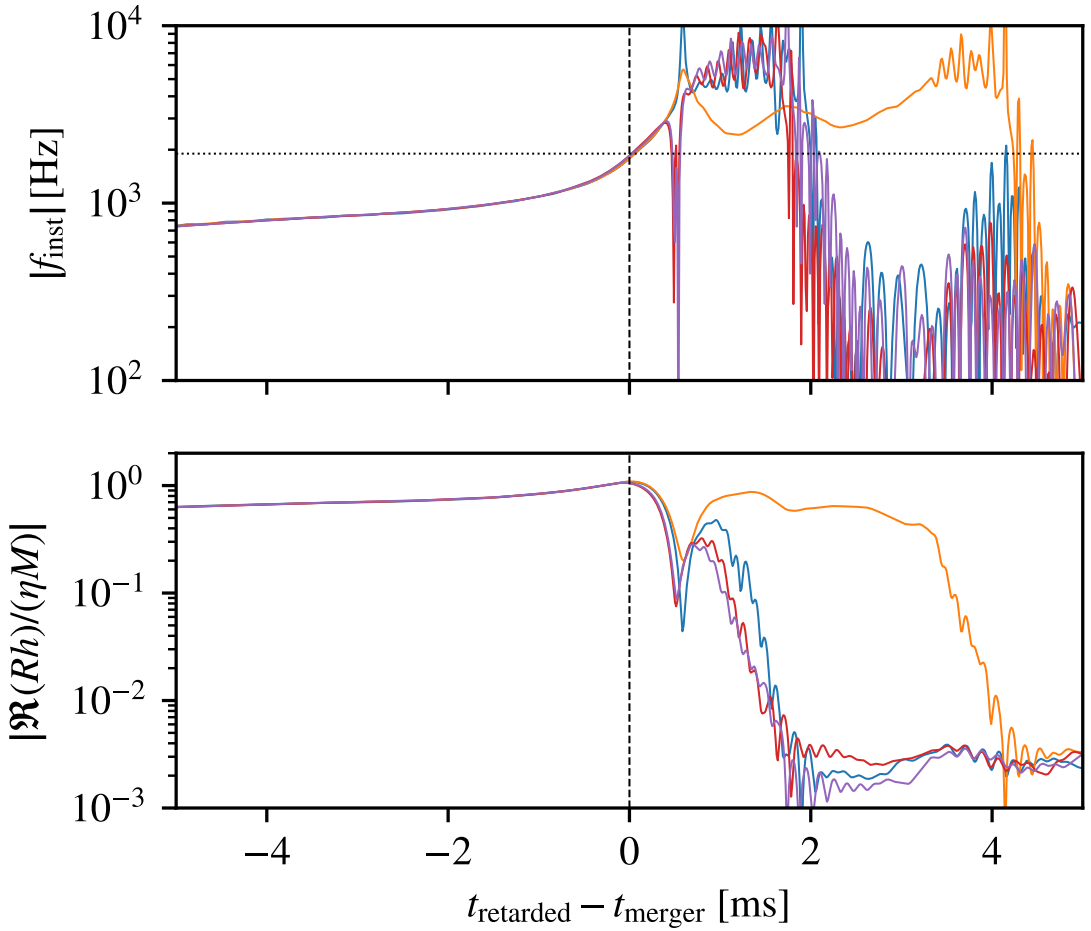

Figure 11: Instantaneous frequency, $f_{\rm inst}$,(top) and gravitational wave strain amplitude, h, (bottom) for the CMF-7-group simulations.

Mismatch

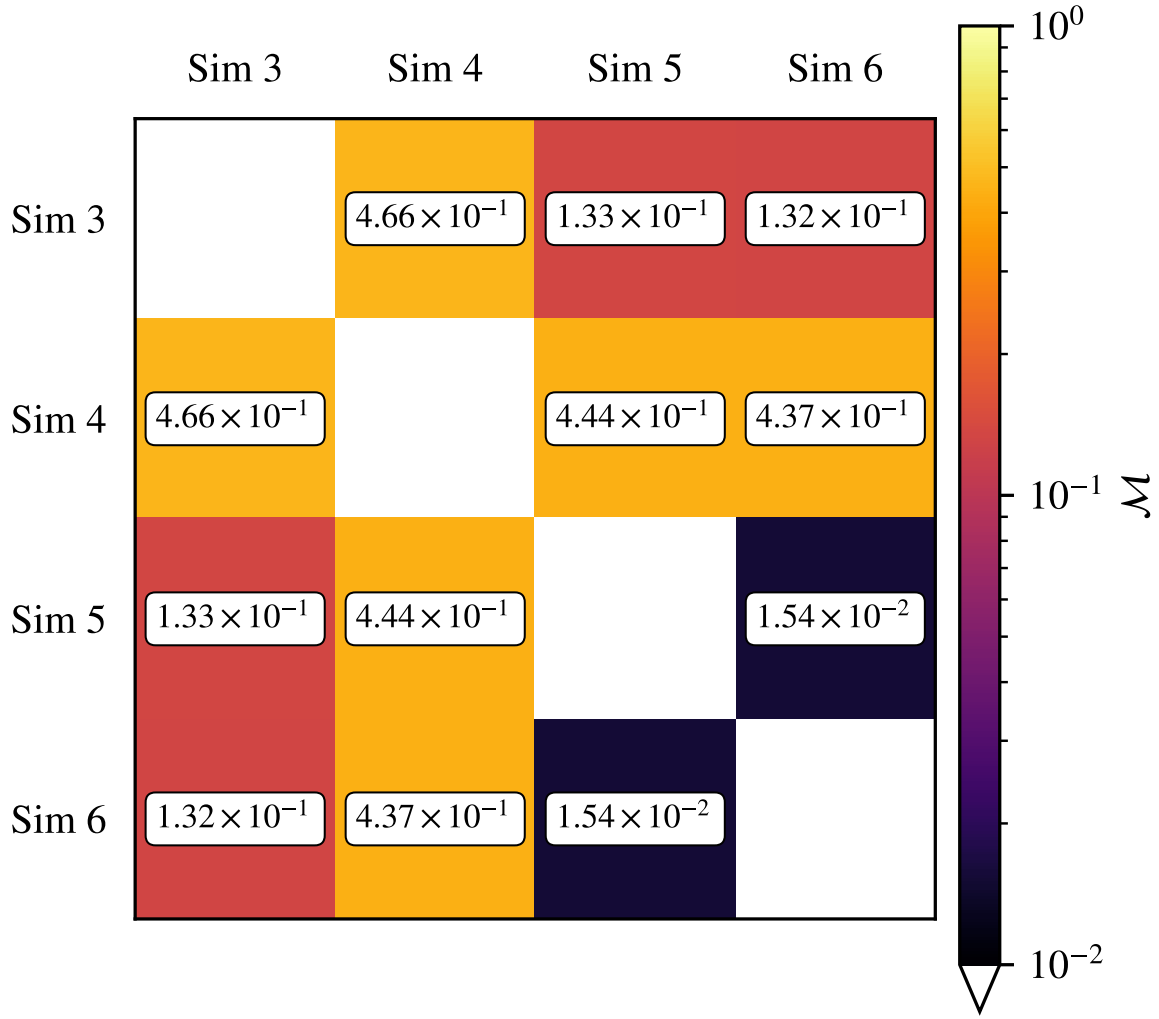

Figure 12: Pair-wise post-merger mismatches for the CMF-7 group of simulations. A frequency of $f_{\text{merger}} = 1.9\,\text{kHz}$ is used to exclude inspiral frequencies from the integrals used in the overlap calculation.

Mismatch

- We can compute from $\mathcal{M}$ the minimum SNR, ϱ, required to distinguish one signal from another through

$$\varrho \geq \frac{1}{\sqrt{2\mathcal{M}}}.$$

- From this we can infer a distinguishability horizon for a given detector.
- For ET-D, the most different signals (highest mismatch, Sim 3 & 4) would be distinguishable out to $\sim$800 Mpc.
- For Cosmic Explorer this grows to $\sim$1200 Mpc.

Modified Equations of State

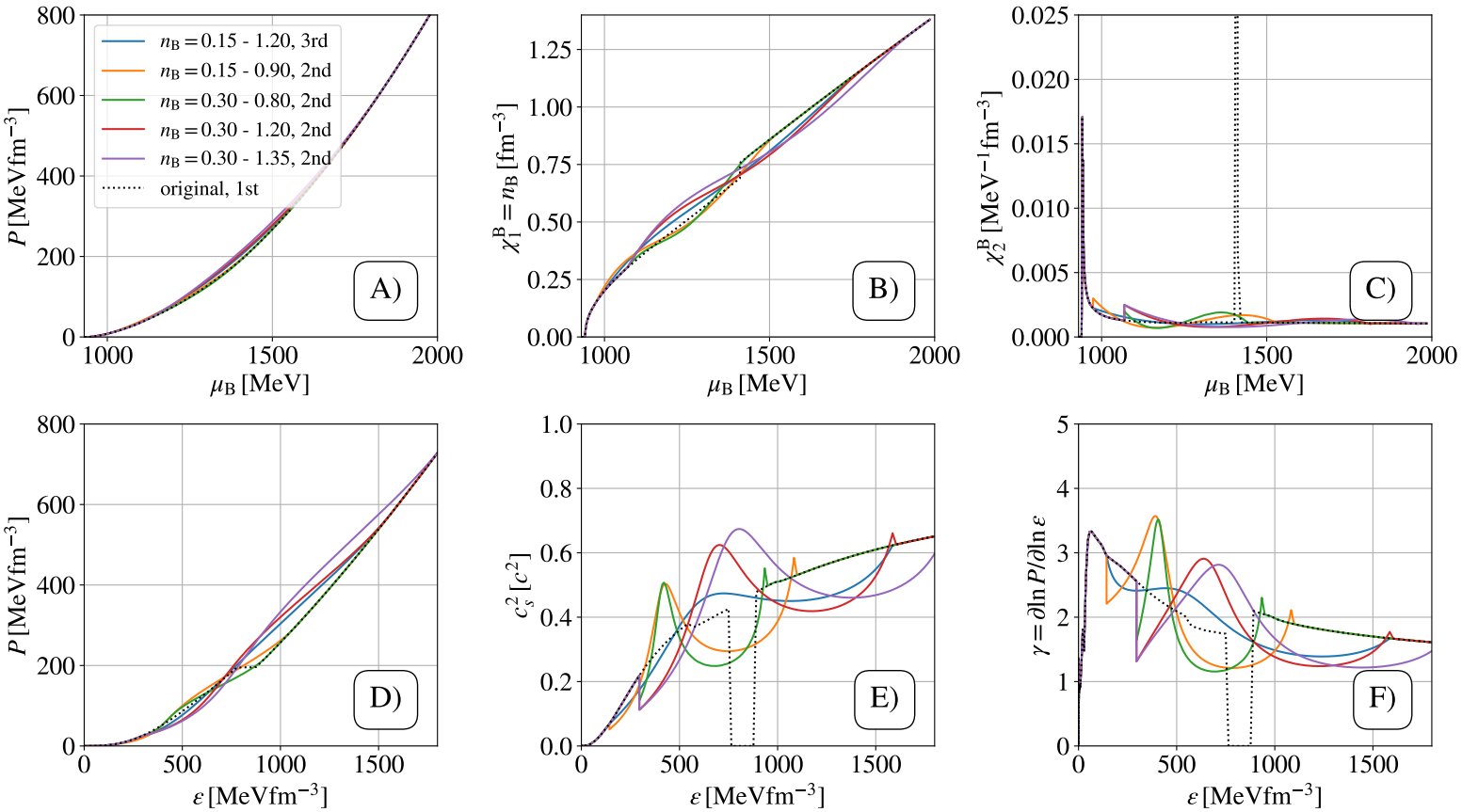

Figure 13: Base CMF-7 equation of state, and several percolated versions.

Density - Stiffness

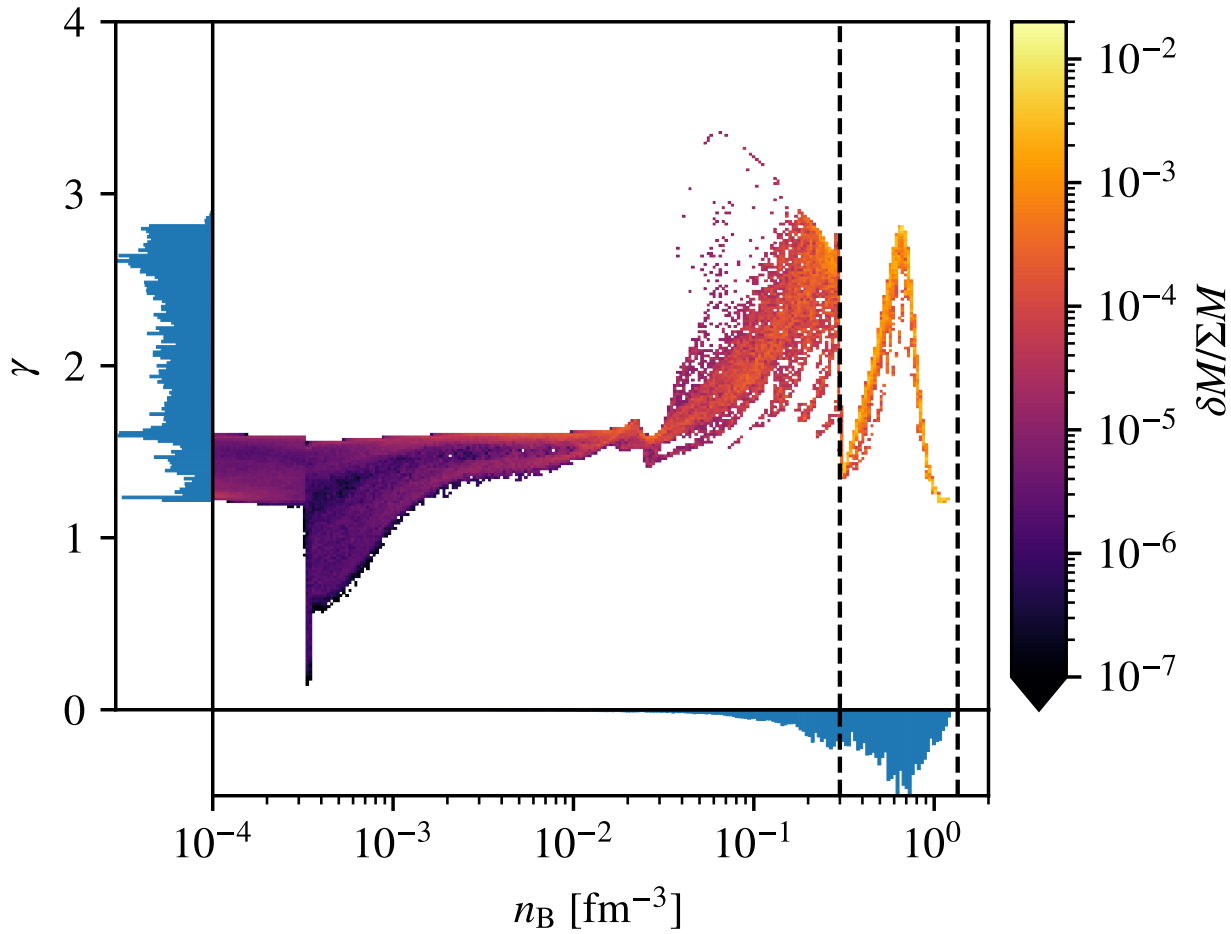

Figure 14: 2-D histogram of density versus adiabatic index γ for CMF-7 model 5 shortly before collapse.

Density - Stiffness

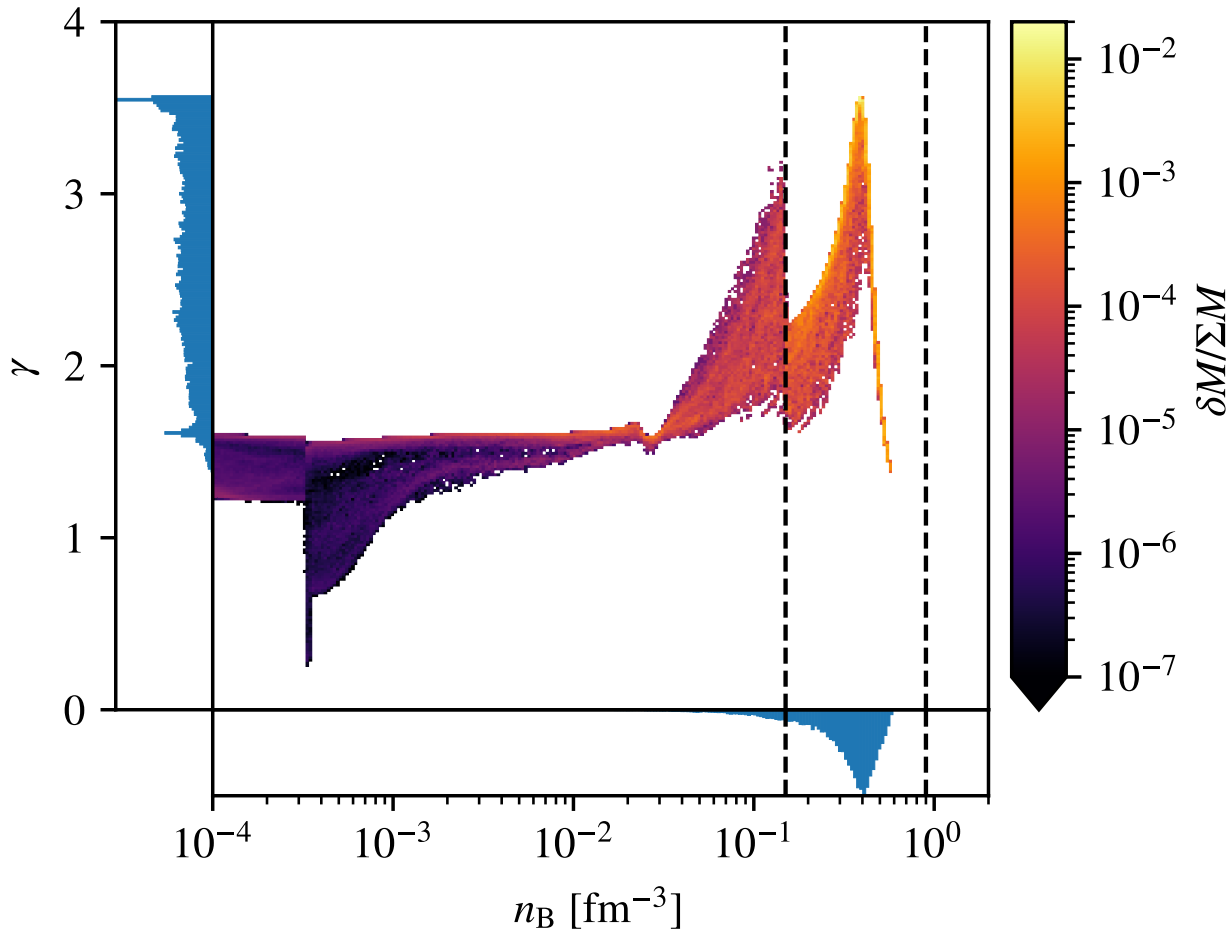

Figure 15: 2-D histogram of density versus adiabatic index γ for CMF-7 model 2 at a sime time after merger as previous plot.

Density - Stiffness

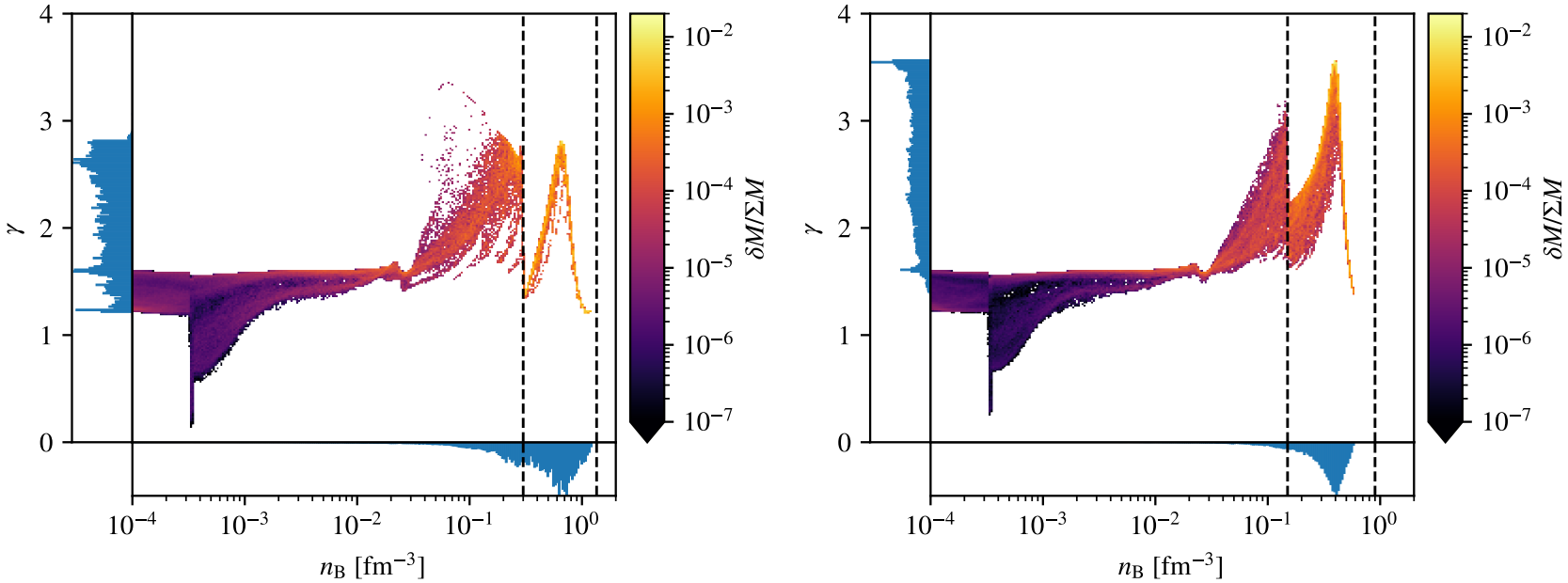

Figure 16: Same as previous two figures—longer lived model on right, prompt collapse on left.

Summary

- We have replaced the first-order phase transition in 3 different quark-hadron EoSs using percolation to achieve higher order phase transitions.
- We have performed simulations of BNS mergers using these constructed EoSs, targeting a crossing point in $M - \Lambda$ space.
- We find that the inspirals match closely, however there are significant differences in post-merger behaviour, detectable with 3G detectors at large distances.

Simulation parameters

Micro EoS	Simulation Number	PT Order	$n_{\mathrm{B,H}}$ [fm^{-3}]	$n_{\mathrm{B,Q}}$ [fm^{-3}]	$\chi^{\mathrm{B}}_{2,\mathrm{H}}$ [fm^{-3}MeV^{-1}]	$\chi^{\mathrm{B}}_{2,\mathrm{Q}}$ [fm^{-3}MeV^{-1}]
CMF-2	1	3	0.15	1.40	–	–
CMF-2	2	2	0.15	0.75	0.0035	0.0015
CMF-7	3	3	0.15	1.20	–	–
CMF-7	4	2	0.15	0.90	0.003	0.001
CMF-7	5	2	0.30	1.20	0.0025	0.001
CMF-7	6	2	0.30	1.35	0.0025	0.001
RDF 1.7	7	2	0.32	0.80	0.0028	0.0009
RDF 1.7	8	2	0.32	1.09	0.0024	0.0012
RDF 1.7	9	2	0.40	0.80	0.0024	0.0009
RDF 1.7	10	2	0.40	1.09	0.0021	0.0012

Simulation parameters contd.

Micro EoS	Simulation Number	M $[M_\odot]$	R [km]	Λ	$n_{\mathrm{B,c}}$ [fm^{-3}]	M_{max} $[M_\odot]$	$n_{\mathrm{B,c,max}}$ [fm^{-3}]
CMF-2	1	1.675	12.7	159.8	0.542	2.00	1.105
CMF-2	2	1.675	12.7	159.9	0.453	2.03	0.956
CMF-7	3	1.500	12.8	333.0	0.470	2.04	1.026
CMF-7	4	1.500	12.8	338.5	0.421	2.07	0.877
CMF-7	5	1.500	12.8	338.6	0.508	2.03	1.062
CMF-7	6	1.500	12.8	328.1	0.528	2.02	1.124
RDF 1.7	7	1.600	11.8	124.4	0.579	2.15	1.047
RDF 1.7	8	1.600	11.8	123.8	0.607	2.14	1.121
RDF 1.7	9	1.675	11.9	98.0	0.606	2.13	1.049
RDF 1.7	10	1.675	11.9	97.7	0.626	2.13	1.122

Recurring Points

- Some EoSs seem to all pass through approximately the same point in M-R and/or M-Λ space.
- We can specialise to 2^{nd} order phase transitions, and introduce variables v_1 and v_2 which set $\mathrm{d}^2p/\mathrm{d}\mu_{\mathrm{B}}^2$ at the percolation boundaries.
- By keeping the other percolation parameters the same, we can vary v_1 and v_2 to explore the vicinity of these recurring points.
- We will look at the effect on the average sound speed squared, given by

$$c_{avg}^2 = \frac{P_c - P_1}{e_c - e_1}.$$

  where 1 denotes quantities at the beinging of the percolation region, and c denotes the centre of the star.
- See arXiv:2506.24069

Recurring Points

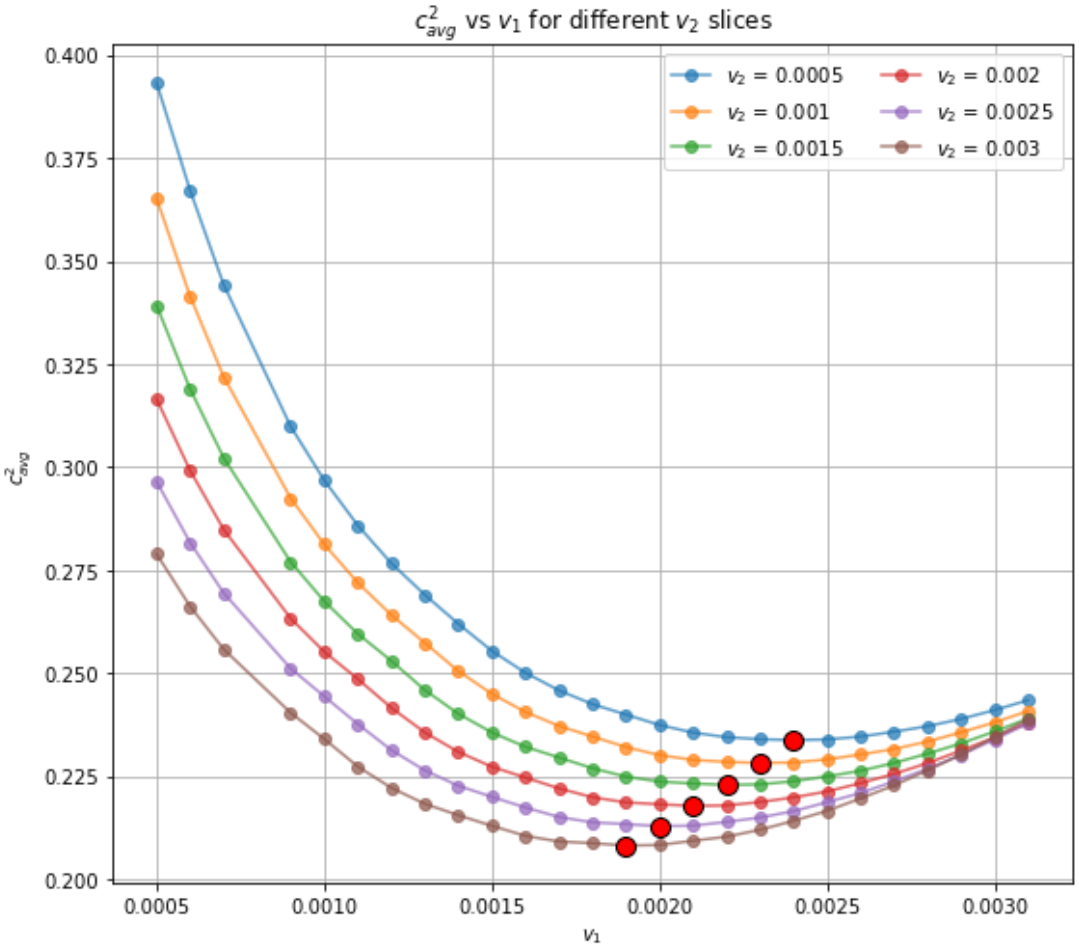

Figure 17: Average sound speed squared for differing v_1 and v_2. Causal minima are highlighted in red.

Recurring Points

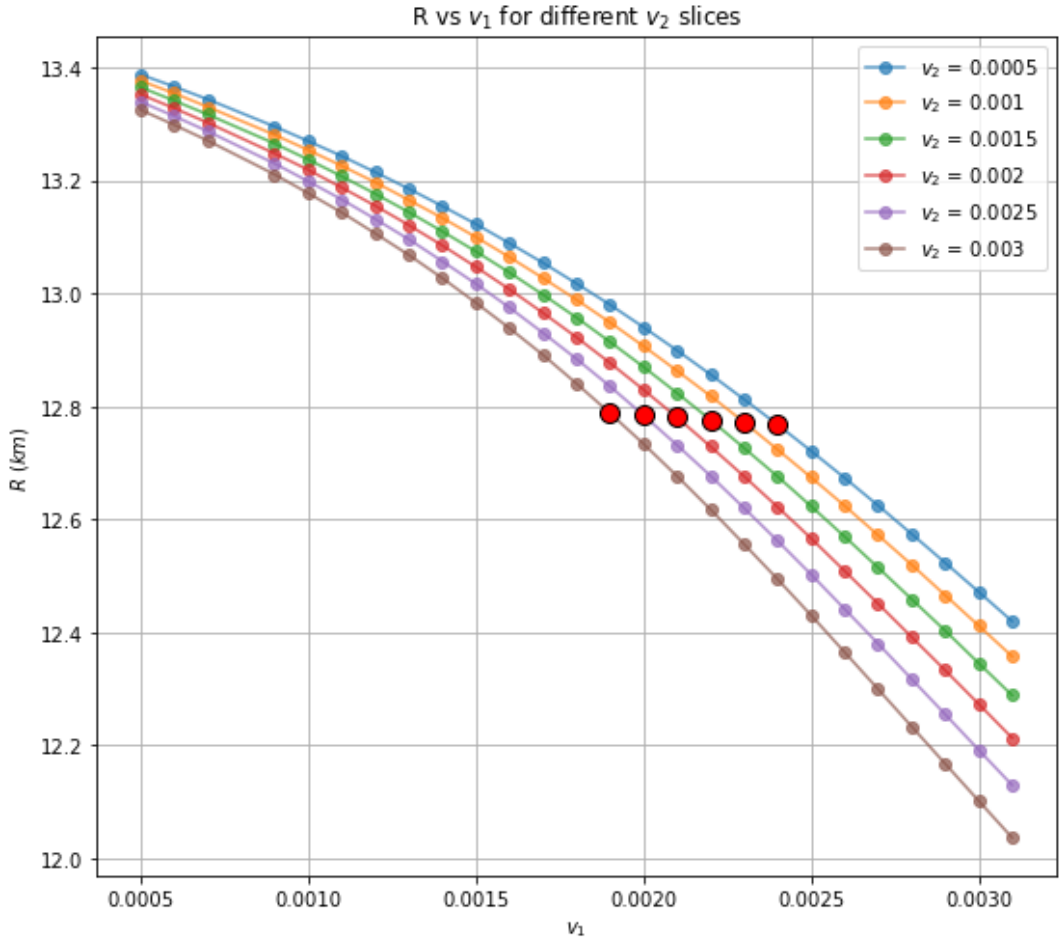

Figure 18: Stellar radius for differing v_1 and v_2. Minima from the previous slide are again highlighted in red.

References I

Bauswein, Andreas et al. (2019). "Identifying a first-order phase transition in neutron star mergers through gravitational waves". In: *Phys. Rev. Lett.* 122.6, p. 061102. DOI: 10.1103/PhysRevLett.122.061102. arXiv: 1809.01116 [astro-ph.HE].

Cook, William et al. (Nov. 2023). "GR-Athena++: General-relativistic magnetohydrodynamics simulations of neutron star spacetimes". In: arXiv: 2311.04989 [gr-qc].

Daszuta, Boris and William Cook (June 2024). "GR-Athena++: magnetohydrodynamical evolution with dynamical space-time". In: arXiv: 2406.05126 [gr-qc].

References II

Espino, Pedro L. et al. (2024). "Revealing phase transition in dense matter with gravitational wave spectroscopy of binary neutron star mergers". In: *Physical Review D* 109.12. DOI: 10.1103/physrevd.109.123009. arXiv: 2301.03619 [astro-ph.HE].

Most, Elias R. et al. (2019). "Signatures of quark-hadron phase transitions in general-relativistic neutron-star mergers". In: *Phys. Rev. Lett.* 122.6, p. 061101. DOI: 10.1103/PhysRevLett.122.061101. arXiv: 1807.03684 [astro-ph.HE].

References III

Prakash, Aviral et al. (2024). "Detectability of QCD phase transitions in binary neutron star mergers: Bayesian inference with the next generation gravitational wave detectors". In: *Physical Review D* 109.10. DOI: 10.1103/physrevd.109.103008. arXiv: 2310.06025 [gr-qc].